Supplementary material

DNA isolation

For fresh frozen tissue samples, DNA was extracted from approximately 25 mg of tissue using the AllPrep DNA/RNA kit (Qiagen Inc, Valencia, CA) as previously described.[1] For archived material, DNA was isolated from five sections of paraffin embedded tissue (each 20 µm), using the QIAamp DNA kit (Qiagen). For the snap frozen biliary brush samples, DNA was isolated using the PrepFiler Forensic DNA Extraction Kit (Applied Biosystems, CA, USA) according to the manufacturer's protocol. Briefly, 500 µl lysis buffer containing DL-Dithiothreitol solution (1M) was added to the Eppendorf tubes containing the brush and were shaken by an Eppendorf thermomixer comfort (Eppendorf, Hamburg, Germany) for 40 min at 70°C. The tubes were centrifuged before removing the brushes. Fifteen µl magnetic beads were added to the supernatant and the reaction was briefly vortexed before adding 300 µl isopropanol. Samples were shaken for 10 min at room temperature. A magnetic stand was used to collect the magnetic beads and the bound DNA, and the samples were subsequently washed three times with wash buffer before they were eluted in 50 µl elution buffer. The ethanol preserved specimens were centrifuged at maximum speed for one min in an Eppendorf centrifuge (Eppendorf Centrifuge model 5415R). The resulting pellets were subjected to vacuum centrifuging for about 30 min to remove all remaining ethanol, before 300 µl lysis buffer was added to the sample and the DNA was isolated using the PrepFiler Forensic DNA Extraction kit (as described above). DNA concentration was determined using the ND-1000 Nanodrop (NanoDrop Technologies, Wilmington, DE).

Functional and expressional aspects of the four individual diagnostic genes

CDO1

Located on 5q23, cysteine deoxygenase type 1 (*CDO1*) has recently been implicated in the development of both non-malignant diseases and cancer (2, 3). It is a non-heme iron dioxygenase regulating the flux between cysteine catabolism and glutathione synthesis, where it oxidizes cysteine to sulfinic acid (2, 4). It is involved in the synthesis of several important metabolic compounds including pyruvate and taurine (5), the latter is a major constituent in bile. In breast cancer, Jeschke *et al.* have reported that *CDO1* is inactivated by DNA promoter hypermethylation in as many as 60% of the cases (4). When *CDO1* expression was restored using a lentiviral approach, the growth and viability of breast

cancer cells were reduced and the cells became sensitive to anthracycline treatment (6). Furthermore, in a study from Peter Jones' lab an epigenetic screen coupled with functional studies performed in colon cancer cell lines showed that inactivating promoter hypermethylation of *CDO1* was important for cell survival, supporting that loss of this gene may have a driver role in tumorigenesis (7). Interestingly, in a study by Prabhu *et al*., metabolomic profiling of 69 patient-derived glioma samples revealed a novel metabolic pathway with increased cysteine sulfinic acid as a result of increased *CDO1* expression (8). By applying a lentiviral-mediated short hairpin RNA approach, they abolished the activity of this pathway *in vivo* in a glioblastoma mouse model. This led to a significant tumor growth inhibition, suggesting that *CDO1* expression may have a different role in gliomas compared to other cancer types. The authors further suggest that this metabolic pathway could serve as a therapeutic target in these aggressive high-grade gliomas (8). In contrast to this, tumor suppressor activity of *CDO1* was recently investigated also by Brait and colleagues in both cell cultures (breast-, colorectal-, esophageal-, gastric-, hepatocellular-, and lung cancer) and mouse models (colorectal cancer). They showed that forced *CDO1* expression markedly reduced tumor cell growth, and conversely that reduced *CDO1* expression increased cell growth, implying a bona fide tumor suppressor function for this gene (3).

CDO1 has been found to be highly expressed in the liver and placenta, but it has also been detected in the brain, heart and pancreas (9). We have previously demonstrated an inverse correlation between DNA promoter methylation and *CDO1* gene expression in a large panel of cell lines from 17 different cancer types, including cholangiocarcinoma. Treating a subset of these cell lines (HCT15, HT29, SW48, and SW480) with epigenetic drugs (5-aza-2'deoxycytidine in combination with trichostatin A) considerably increased the *CDO1* expression (10), underscoring that DNA promoter methylation is a likely regulator of *CDO1* expression. Analyzing sample series from cholangiocarcinoma, colorectal-, gastric-, and pancreatic cancer, we further demonstrated that the promoter region of *CDO1* was frequently methylated across several cancer types (1, 10). In line with this, the previously mentioned Brait study showed a similar high methylation frequency in colorectal- and gastric cancer (*ca*. 90%), in addition to bladder-, breast-, esophagus-, and lung cancer. By analyzing the expression of *CDO1* in these cancer types, significant repression was identified at both the RNA and protein level in tumors (3). In an effort to identify novel diagnostic biomarkers for non-small cell lung cancer, Wrangle and colleagues recently used epigenetic drug treatment of cell lines as well as a large publically available

database and patient material. A three-gene biomarker panel including *CDO1* was identified. They reported a sensitivity of up to 99% and a complete specificity of 100% (11).

In the current study, we have obtained gene expression data (RNA seq) from The Cancer Genome Atlas (TCGA; Supplementary figure 1). In concordance with the generally high methylation frequency (77%) that we report here, a significant reduction in *CDO1* expression was observed in cholangiocarcinomas compared with non malignant controls. A direct causation of the presence of promoter DNA methylation and reduced *CDO1* gene expression cannot be confirmed for cholangiocarcinomas at this point since these analyses have been performed in different samples. However, based on the combined scientific data presented above is not unlikely that *CDO1* is epigenetically regulated also in cholangiocarcinomas.

CNRIP1

Cannabinoid receptor interacting protein 1 (*CNRIP1*), located on 2p14, is encoding a protein that interacts with the C-terminal end of the cannabinoid receptor 1 (12). *CNRIP1* was annotated as an open reading frame (*C2orf32*) until the genome assembly hg18 in 2006, and so far little is known about the function of this protein in general and its potential role in cancer in particular. Also in 2006, *CNRIP1* was identified as a promoter DNA methylation target gene in colorectal cancer (13), and later we demonstrated that it was frequently methylated also in adenomas (14). Recently, *CNRIP1* was reported to be hypermethylated in Non-Hodgkins Lymphomas (15), where it is associated with worse overall survival in patients with diffuse large B-cell lymphoma. In line with *CDO1*, we have previously demonstrated an inverse correlation between *CNRIP1* mRNA expression and promoter methylation in a panel of cancer cell lines (14). Such an association could also be seen in colorectal cancer tissue samples, although not equally strong (11). When cell lines harbouring promoter DNA methylation of *CNRIP1* were treated with epigenetic drugs (5-aza-2'deoxycytidine and trichostatin A), the gene expression increased several folds (11) underscoring that the methylation may affect the gene expression. However, this was not supported in an array-based study where intermediate expression levels of *CNRIP1* was maintained in the presence of cancer specific methylation in a small set of colorectal tumors (16). Recently, aberrantly methylated *CNRIP1* was identified also in diffuse-type gastric carcinomas (17), supporting the notion of similarities across gastrointestinal malignancies (3,

10, 18-20). Here, we report a frequent *CNRIP1* methylation of 82% in cholangiocarcinomas. Since the TCGA RNA Seq-data (Supplementary Figure 1) depict a low *CNRIP1* expression in the control samples, a transcriptional reduction in CCAs cannot be observed. Interestingly, we have previously shown that *CNRIP1* is methylated in 40% of normal appearing mucosa samples taken at a distance from a colorectal cancer, indicating an epigenetic field defect (14). It cannot be ruled out that the matching controls included in the TCGA data set also are affected by such a field defect.

Although the role of this gene tumorigenesis in general remains to be fully understood, the high methylation frequency identified also in cholangiocarcinomas suggest a biomarker role for *CNRIP1* in gastrointestinal cancers

SEPT9

SEPT9 is located on 17q25, and is a member of a large family of septin proteins involved in cytokinesis and cell cycle control and it has multiple distinct transcripts which play important physiological roles, including in actin dynamics, angiogenesis, cell motility, proliferation, and microtubule regulation (21, 22). It is suggested that *SEPT9* is included in multisubunit heteromers and is critical for final separation of daughter cells during cytokinesis (23), and a compromised transcription of *SEPT9* may influence the septin heteromer complex. Moreover, knockout of *SEPT9* has been shown to be lethal in mouse embryos (24). In cancer, *SEPT9* has been implicated in the development of malignancies of various tissues, including breast, colon, ovary, head and neck, and cells of the immune system (25-31). Promoter hypermethylation of *SEPT9* is already established as a clinical biomarker for detecting colorectal cancer using circulating DNA. Recently, a large prospective international study (The PRospective Evaluation of SEPTin 9 (PRESEPT) study) addressed its performance in almost 8000 asymptomatic patients. Across all stages, a sensitivity of 48% and a specificity of 92% were reported (29). It was also recommended to improve the sensitivity for early cancers before utilization as a population screening test (32).

In colorectal cancer, a significant inverse correlation between *SEPT9* promoter methylation and mRNA expression has been demonstrated and is proposed to account for the progression from benign to malignant lesion (33). However, overexpression of various *SEPT9* isoforms have been shown across

several studies including breast-, prostate-, ovarian-, and hepatic cancer. This is probably a result of DNA methylation at alternative promoters and/or genomic amplification, suggestive of aberrant expression of *SEPT9* isoforms in a tissue specific manner (21, 27, 30, 34, 35). In line with this, we observe an up-regulation of *SEPT9* in TCGA data in cholangiocarcinomas compared to the controls (supplementary figure 1). However, since we only observed 26% methylation of *SEPT9* in our cholangiocarcinoma samples, this increase in expression could be the contribution of the unmethylated tumors. This underscores that the molecular mechanisms regarding *SEPT9* expression and its role in cholangiocarcinoma should be further studied.

VIM

VIM, located on 10p13, encodes a member of the intermediate filament family and the protein is involved in the maintenance of cell shape, integrity of the cytoplasm and stabilization of cytoskeletal interactions (36). It has also been shown to be involved in immune response (37), transport of low-density lipoprotein (38), and seems to function as an organizer of critical proteins involved in attachment, migration, and cell signalling (39, 40). Expression of *VIM* has been identified in mesenchymal cell types including fibroblasts and endothelial cells, as well as pancreatic and neural precursor cells (reviewed in (41)). In cancer, *VIM* is considered to have a pivotal role in the epithelial-to-mesenchymal transition and thereby in cells undergoing invasion and metastasis (42). Moreover, promoter methylation of *VIM* has been identified in several cancer types, including bladder, breast, cervical, colorectal, gastric, hepatocellular, esophageal, and pancreas (18, 43-48). For colorectal cancer, the frequent methylation of *VIM* is established and included in a non-invasive test using stool (41, 49, 50). Importantly, studies have shown that *VIM* has lost its expression already in normal colonic cells (51, 52). In concordance with this, a very low *VIM* expression is seen in both control samples and tumors from the TCGA data (supplementary figure 1). This implies that the silencing of *VIM* happens early and that the subsequent promoter hypermethylation in cancer may be a way to stably maintain this inactivation.

Supplementary Table 1. Clinico-pathological features for fresh frozen and archival CCA samples

Sample series	Tumor diagnosis	Liver disease	Tissue origin	Cancer status	Age	Gender	Operative procedure
Fresh frozen	CCA	PSC	ECC	Tumor in main bile duct. Lymph node metastasis near coeliac artery	50	M	Laparoscopy
Fresh frozen	CCA	None	ECC	Tumor in common hepatic duct, 25 mm	72	M	Liver resection
Fresh frozen	CCA	None	ECC	Hilar tumor, 32 mm	66	F	Liver transplantation (Mayo protocol)
Fresh frozen	CCA	None	ECC	Tumor in common hepatic duct, 20 mm. Perineural- and vascular infiltration. Lymph node metastases	67	F	Liver resection
Fresh frozen	CCA	None	ECC	Hilar tumor, 30 mm. Infiltration in liver tissue. Lymph node metastases	60	F	Liver transplantation (Mayo protocol)
Fresh frozen[#]	CCA	None	ECC	Adenocarcinoma	70	F	Liver resection
Fresh frozen[#]	CCA	None	ECC	Adenocarcinoma	65	F	Liver resection
Fresh frozen[#]	CCA	None	ECC	Adenocarcinoma	61	M	Liver resection
Fresh frozen[#]	CCA	None	ECC	Adenocarcinoma	73	M	Liver resection
Fresh frozen	CCA	None	ECC	Hilar tumor. Perineural infiltration	47	F	Laparotomy
Fresh frozen	CCA	PSC	ECC	Hilar tumor, 60 mm. Liver tissue-, perineural- and vascular infiltration	43	M	Liver resection
Fresh frozen	CCA	None	ECC	Tumor in main bile duct, 25 mm. Infiltration in pancreas, duodenum and ampulla Vateri	76	F	Whipple`s operation
Fresh frozen	CCA	None	ICC	Intrahepatic tumor, too large for planned resection with auto-transplantation	31	F	Laparotomy
Archive[*]	CCA	PSC	ECC	Lymph node metastases in hepatoduodenal ligament	53	M	Laparotomy
Archive[*]	CCA	PSC	ECC	Lymph node metastases in hepatoduodenal ligament	53	M	Laparotomy
Archive	CCA	PSC	ECC	Hilar tumor, 18 mm	46	M	Liver transplantation
Archive	CCA	PSC	ECC	Tumor in main bile duct. Perineural- and fatty tissue infiltration	43	M	Liver transplantation
Archive[*]	CCA	PSC	ECC	Tumor in main bile duct. Perineural- and fatty tissue infiltration	50	M	Liver transplantation
Archive[*]	CCA	PSC	ECC	Tumor in main bile duct. Perineural- and fatty tissue infiltration	50	M	Liver transplantation
Archive	CCA	PSC	ECC	Extrahepatic bile duct and pancreatic tissue with adenocarcinoma infiltration	54	M	Liver transplantation
Archive[*]	CCA	PSC	ICC	Intrahepatic tumor, 100 mm. Lymph node metastasis	32	M	Liver resection

Archive*	CCA	PSC	ICC	Intrahepatic tumor, 100 mm. Lymph node metastasis	32	M	Liver resection
Archive	CCA	None	ECC	Hilar tumor, 30 mm. Liver tissue infiltration. Lymph node metastasis	61	F	Liver transplantation (Mayo protocol)
Archive*	CCA	None	ICC	Intrahepatic tumor, 30 mm. Perineural- and vascular infiltration. Lymph node metastasis	47	M	Liver transplantation
Archive*	CCA	None	ICC	Intrahepatic tumor, 30 mm. Perineural- and vascular infiltration. Lymph node metastasis	47	M	Liver transplantation
Archive	CCA	PSC	ECC	Adenocarcinoma infiltrating liver-, connective- and fatty tissue	49	M	Laparotomy
Archive*	CCA	PSC	ICC	Tumor in left hepatic duct. Perineural- and perimuscular infiltration	43	M	Liver transplantation
Archive*	CCA	PSC	ICC	Tumor in left hepatic duct. Perineural- and perimuscular infiltration	43	M	Liver transplantation
Archive	CCA	PSC	ICC	Adenocarcinoma infiltrating connective tissue (lig. falciforme)	65	M	Laparotomy
Archive*	CCA	PSC	ECC	Hilar tumor. Perineural- and perivascular infiltration. Lymph node metastasis	54	M	Liver transplantation
Archive*	CCA	PSC	ECC	Hilar tumor. Perineural- and perivascular infiltration. Lymph node metastasis	54	M	Liver transplantation
Archive	CCA	PSC	ECC	Tumor in main bile duct and hepatic duct. Perineural- and vascular infiltration. Lymph node metastasis	38	M	Whipple`s operation
Archive*	CCA	None	ECC	Tumor in common hepatic duct, 25 mm	72	M	Liver resection
Archive*	CCA	None	ECC	Tumor in common hepatic duct, 25 mm	72	M	Liver resection
Archive*	CCA	None	ECC	Tumor in common hepatic duct, 25 mm	72	M	Liver resection
Archive	CCA	None	ECC	Hilar tumor, 45 mm. Perineural infiltration	61	M	Liver transplantation
Archive*	CCA	None	ECC	Tumor in common hepatic duct, right and left hepatic ducts, 20 mm. Perineural- and vascular infiltration. Lymph node metastasis	67	F	Liver resection
Archive*	CCA	None	ECC	Tumor in common hepatic duct, right and left hepatic ducts, 20 mm. Perineural- and vascular infiltration. Lymph node metastasis	67	F	Liver resection
Archive	CCA	None	ECC	Distal common bile duct. Infiltration through wall into connective and fatty tissue. Perineural infiltration	70	F	Liver transplantation

All CCA samples are grouped according to their respective sample series, fresh frozen and archival samples. #Tumor samples are provided by Imperial College, London, UK. All other tumor samples are derived from Oslo University Hospital, Rikshospitalet, Oslo, Norway. *Samples are derived from the same patient when they appear in a vertical sequential manner. Abbreviations: CCA, cholangiocarcinoma; ECC, extrahepatic cholangiocarcinoma; F, female; ICC, intrahepatic cholangiocarcinoma; M, male; PSC, primary sclerosing cholangitis.

Supplementary Table 2. Clinico-pathologic features for non-malignant tissue samples

Sample series	Tumor diagnosis	Liver disease	Tissue origin	Age	Gender
Fresh frozen	Non-malignant	PSC	Peripheral liver	60	M
Fresh frozen	Non-malignant	PSC	Peripheral liver	63	M
Fresh frozen	Non-malignant	PSC	Peripheral liver	23	M
Fresh frozen	Non-malignant	PSC	Peripheral liver	35	M
Fresh frozen	Non-malignant	PSC	Peripheral liver	31	M
Fresh frozen	Non-malignant	PSC	Peripheral liver	32	M
Fresh frozen	Non-malignant	PSC	Peripheral liver	57	M
Fresh frozen	Non-malignant	PSC	Peripheral liver	36	F
Fresh frozen	Non-malignant	PSC	Peripheral liver	44	F
Fresh frozen	Non-malignant	Alcohol	Peripheral liver	57	M
Fresh frozen	Non-malignant	Alcohol	Peripheral liver	59	M
Fresh frozen	Non-malignant	Alcohol	Peripheral liver	48	M
Fresh frozen	Non-malignant	PBC	Peripheral liver	40	F
Fresh frozen	Non-malignant	PBC	Peripheral liver	69	F
Fresh frozen	Non-malignant	Hemochromatosis	Peripheral liver	51	M
Fresh frozen	Non-malignant	AIH	Peripheral liver	43	F
Fresh frozen	Non-malignant	AIH	Peripheral liver	32	F
Fresh frozen	Non-malignant	PBC	Peripheral liver	72	F
Fresh frozen	Non-malignant	Alcohol	Peripheral liver	51	M
Fresh frozen	Non-malignant	Alcohol	Peripheral liver	59	M
Fresh frozen	Non-malignant	Cryptogenic cirrhosis	Peripheral liver	62	M
Archive	Non-malignant	PSC	Peripheral liver*	43	M
Archive	Non-malignant	PSC	Peripheral liver*	43	M
Archive	Non-malignant	None	Peripheral liver*	47	M

Archive	Non-malignant	PSC	Extrahepatic bile duct	17	F
Archive	Non-malignant	PSC	Peripheral liver	17	F
Archive	Non-malignant	PSC	Hilum of the liver	17	F
Archive	Non-malignant	None	Peripheral liver*	67	F
Archive	Non-malignant	AIH	Peripheral liver	45	F
Archive	Non-malignant	AIH	Hilum of the liver	45	F
Archive	Non-malignant	None	Peripheral liver*	60	F
Archive	Non-malignant	PSC	Extrahepatic bile duct	27	M
Archive	Non-malignant	PSC	Peripheral liver	27	M
Archive	Non-malignant	PSC	Hilum of the liver	27	M
Archive	Non-malignant	PSC	Peripheral liver*	54	M
Archive	Non-malignant	PSC	Peripheral liver	71	F
Archive	Non-malignant	PSC	Extrahepatic bile duct	71	F
Archive	Non-malignant	PSC	Hilum of the liver	71	F
Archive	Non-malignant	PSC	Peripheral liver*	43	M
Archive	Non-malignant	PSC	Hilum of the liver	65	M
Archive	Non-malignant	PSC	Peripheral liver	65	M
Archive	Non-malignant	PSC	Peripheral liver*	46	M
Archive	Non-malignant	PBC	Extrahepatic bile duct	59	F
Archive	Non-malignant	PBC	Hilum of the liver	59	F
Archive	Non-malignant	PBC	Peripheral liver	59	F
Archive	Non-malignant	AIH	Peripheral liver	43	F
Archive	Non-malignant	PSC	Hilum of the liver	40	M
Archive	Non-malignant	PSC	Central liver	40	M
Archive	Non-malignant	Alcohol	Hilum of the liver	57	M
Archive	Non-malignant	PSC	Extrahepatic bile duct	60	M
Archive	Non-malignant	PSC	Hilum of the liver	60	M

Archive	Non-malignant	PSC	Peripheral liver	60	M
Archive	Non-malignant	PBC	Peripheral liver	40	F
Archive	Non-malignant	AIH	Hilum of the liver	32	F

All non-malignant samples are grouped according to their respective sample series, fresh frozen and archival samples. Samples are derived from the same patient when they appear in a vertical sequential manner joint by a line. *Sample from explanted liver, from unaffected region distant from CCA. Abbreviations: AIH, autoimmune hepatitis; F, female; M, male; PBC, primary biliary cholangitis; PSC, primary sclerosing cholangitis. All non-malignant tissue samples are derived from Oslo University Hospital, Rikshospitalet, Oslo, Norway.

Supplementary Table 3. Clinico-pathologic features for biliary brush samples

Sample series	Sample number	Tumor diagnosis	Liver disease	Tissue origin	Cancer status	Cytology score	Age	Gender	Operative procedure
Biliary brush	1a	CCA	PSC	ECC	Lymph node metastases in hepatoduodenal ligament	1 (N/D)	40	M	Laparotomy
Biliary brush	1b	CCA	PSC	ECC	Lymph node metastases in hepatoduodenal ligament	1 (N/D)	40	M	Laparotomy
Biliary brush	2	CCA	None	ECC	CT/PET scan and ERCP compatible with cholangiocarcinoma. Lymph node metastasis (cytology)	5	35	M	None
Biliary brush	3	CCA	PSC	ICC	CT/PET scan and ERCP compatible with cholangiocarcinoma. Skeletal metastases. No biopsy	4	53	M	None
Biliary brush	4a	CCA	None	ECC	Tumor in distal main bile duct. Connective tissue-, fatty tissue- and perineural infiltration	2	70	F	Liver transplantation
Biliary brush	4b	CCA	None	ECC	Tumor in distal main bile duct. Connective tissue-, fatty tissue- and perineural infiltration	N/A	70	F	Liver transplantation
Biliary brush	5	CCA	PSC	ECC	Tumor in main bile duct and hepatic duct. Perineural- and vascular infiltration. Lymph node metastasis	5 and 3*	38	M	Whipple`s operation
Biliary brush	6	CCA	None	ECC	Hilar tumor, 30 mm. Liver tissue infiltration. Lymph node metastasis	4	60	F	Liver transplantation (Mayo protocol)
Biliary brush	7	CCA	None	ECC	Hilar tumor. Perineural infiltration	1 (N/C)	47	F	Laparotomy
Biliary brush	8	CCA	PSC	ECC	Tumor in main bile duct. Lymph node metastasis	5	50	M	Laparoscopy
Biliary brush	9	CCA	PSC	ICC	Intrahepatic tumor, 15 mm, close to the hilum	4	55	M	Liver transplantation

Biliary brush	10a	CCA	PSC	ICC	Intrahepatic tumor, 100 mm. Lymph node metastasis	N/A	32	M	Liver resection
Biliary brush	10b	CCA	PSC	ICC	Intrahepatic tumor, 100 mm. Lymph node metastasis	N/A	32	M	Liver resection
Biliary brush	11	CCA	PSC	ECC	Hilar tumor, 60 mm. Liver tissue-, perineural- and vascular infiltration	1 (N/D)	43	M	Liver resection
Biliary brush	12	CCA	None	ECC	Hilar tumor, 32 mm	4 and 3*	66	F	Liver transplantation (Mayo protocol)
Biliary brush	13	CCA	PSC	ICC	Intrahepatic tumor 50 mm. Lymph node metastasis (cytology)	5	66	M	None
Biliary brush	14	CCA	Not typical PSC	ICC/ECC	CT: suspicious intrahepatic tumor. PET scan: compatible with CCA in common hepatic duct and main bile duct. Lymph node metastasis (cytology)	5	35	M	None
Biliary brush	15	CCA	PSC	ICC and hilum	Lymph node metastases	4	40	M	Laparotomy
Biliary brush	16	CCA	PSC	ICC and hilum	CT/PET scan compatible with CCA with lymph node metastases. Suspected skeletal metastases. No biopsy	4	53	M	None
Biliary brush	17	CCA	PSC	ICC	Intrahepatic CCA in explanted liver. BilIN 3 in extrahepatic bile duct close to the hilum	3	56	M	Liver transplantation
Biliary brush	18a	CCA	PSC	ECC	Hilar tumor, 50 mm x 17 mm. Lymph node metastasis.	4	55	M	Liver transplantation
Biliary brush	18b	CCA	PSC	ECC	Hilar tumor, 50 mm x 17 mm. Lymph node metastasis.	4	55	M	Liver transplantation
Biliary brush	19	CCA	None	ECC	Biopsy via percutaneous transhepatic cholangiography	5	82	F	None
Biliary brush	20a	CCA	None	Hilar	Hilar tumor, 32 mm	5	66	F	Liver transplantation (Mayo protocol)
Biliary brush	20b	CCA	None	Hilar	Hilar tumor, 32 mm	5	66	F	Liver transplantation (Mayo protocol)
Biliary brush	21	CCA	None	ECC	Lymph node metastasis	5	48	M	Laparotomy
Biliary brush	22	CCA	PSC	ICC	Liver biopsy with infiltration of adenocarcinoma	5	43	M	None
Biliary brush	23	CCA	None	Hilum	Hilar tumor by MRCP and ERCP. No biopsy	5	47	F	None
Biliary brush	24	CCA	None	ECC and hilar	Peritoneal metastasis (biopsy)	5	64	M	None
Biliary brush	25	CCA	None	ECC and hilar	ERCP with biopsy	5	77	M	None
Biliary brush	26a	CCA	Noe	Hilum	Hilar tumor by MRCP, CT and ERCP. No biopsy	5	75	M	None

Biliary brush	26b	CCA	None	Hilum	Hilar tumor by MRCP, CT and ERCP. No biopsy	5	75	M	None
Biliary brush	27	CCA	None	ECC	Tumor in distal extrahepatic bile duct with infiltration into pancreas and duodenum	5	69	F	Whipple`s operation
Biliary brush	28	CCA	None	ECC	ERCP compatible with CCA. No biopsy	5	83	F	None
Biliary brush	29	CCA	None	ECC	Tumor in distal extrahepatic bile duct with infiltration into pancreas, duodenum and papilla Vateri	5	79	M	Whipple`s operation
Biliary brush	30	CCA	PSC	ECC	Lymph node metastases	5	35	M	Laparotomy
Biliary brush	31	CCA	PSC	ICC	Tumor, 70 mm, right liver lobe. Biopsy	2	61	M	None
Biliary brush	32	CCA	PSC	Hilar	Lymph node metastases	3	53	M	Liver transplantation
Biliary brush	33	CCA	None	ICC and hilum	Liver biopsy with infiltration of adenocarcinoma. Lymph node metastases	1 (N/D)	61	F	None
Biliary brush	34	CCA	None	Hilar	CT, ERCP and MRCP compatible with CCA. No biopsy	N/A	64	M	None
Biliary brush	35	CCA	PSC	ICC and hilum	CT and ERCP compatible with CCA. No biopsy	2	71	M	None
Biliary brush	36	CCA	PSC	Peritoneum	ERCP compatible with CCA. Peritoneal carcinomatosis	1 (N/C)	71	M	Laparotomy
Biliary brush	37a	CCA	PSC	ICC and hilum	Lymph node metastases	3	56	M	Liver resection
Biliary brush	37b	CCA	PSC	ICC and hilum	Lymph node metastases	4	56	M	Liver resection
Biliary brush	38	CCA	PSC	ICC	Tumor, 90 mm, right liver lobe. Biopsy	2	43	M	None
Biliary brush	39	CCA	PSC	Hilar	Lymph node metastases	N/A	55	F	Laparotomy
Biliary brush	40	CCA	PSC	Hilar	Intrahepatic metastases	3	55	F	Laparotomy
Biliary brush	41	CCA	PSC	Hilar	Lymph node metastasis	4	40	M	Liver transplantation
Biliary brush	42	CCA	PSC	ECC	Peritoneal carcinomatosis	2	41	M	Laparotomy
Biliary brush	1	GBC	PSC	Gall bladder	Lymph node metastasis	2	58	M	Laparotomy
Biliary brush	2	GBC	None	Gall bladder	Peritoneal metastases	5	59	M	Laparotomy
Biliary brush	3	GBC	None	Gall bladder	Lymph node metastases	2	79	F	Laparotomy
Biliary brush	4	GBC	PSC	Gall bladder	Lymph node metastases	2	54	M	Laparotomy
Biliary brush	5	GBC	PSC	Gall bladder	Gall bladder adenocarcinoma with local infiltration	3	67	M	Liver transplantation
Biliary brush	1	PC	None	ECC or pancreas	Tumor in caput pancreatis	5	48	M	Laparotomy

Biliary brush	2	PC	None	Pancreas	Pancreatic cancer with liver and lung metastases. Biopsy from tumor and lung metastasis	5	63	M	None
Biliary brush	3a	PC	PSC	Pancreas	Lymph node metastasis	2	60	M	Laparotomy
Biliary brush	3b	PC	PSC	Pancreas	Lymph node metastasis	3	60	M	Laparotomy

									Follow up (months)
Biliary brush	1	Non-malignant	PSC	-	-	2	36	M	36
Biliary brush	2	Non-malignant	PSC	-	-	2	26	F	43
Biliary brush	3	Non-malignant	PSC	-	-	3	34	M	41
Biliary brush	4	Non-malignant	PSC	-	-	2	24	M	24
Biliary brush	5	Non-malignant	PSC	-	-	2	38	M	41
Biliary brush	6	Non-malignant	PSC	-	-	2	35	M	41
Biliary brush	7	Non-malignant	PSC	-	-	2	45	M	49
Biliary brush	8	Non-malignant	PSC	-	-	2	35	M	34
Biliary brush	9	Non-malignant	PSC	-	-	2	46	F	41
Biliary brush	10	Non-malignant	PSC	-	-	2	37	M	42
Biliary brush	11	Non-malignant	PSC	-	-	2	36	F	43
Biliary brush	12	Non-malignant	PSC	-	-	2	18	M	49
Biliary brush	13	Non-malignant	PSC	-	-	2	43	M	40
Biliary brush	14	Non-malignant	PSC	-	-	2	40	F	47
Biliary brush	15	Non-malignant	PSC	-	-	2	46	M	45
Biliary brush	16	Non-malignant	PSC	-	-	2	41	M	24
Biliary brush	17	Non-malignant	PSC	-	-	2	27	M	43
Biliary brush	18	Non-malignant	PSC	-	-	2	31	M	42
Biliary brush	19	Non-malignant	PSC	-	-	2	43	F	47
Biliary brush	20	Non-malignant	PSC	-	-	2	18	M	49

Biliary brush	21	Non-malignant	PSC	-	-	2	53	F	13
Biliary brush	22a	Non-malignant	PSC	-	-	2	50	M	31
Biliary brush	22b	Non-malignant	PSC	-	-	2	50	M	31
Biliary brush	23	Non-malignant	PSC	-	-	2	59	M	36
Biliary brush	24a	Non-malignant	PSC	-	-	2	49	M	44
Biliary brush	24b	Non-malignant	PSC	-	-	2	49	M	44
Biliary brush	25	Non-malignant	PSC	-	-	2	27	M	57
Biliary brush	26	Non-malignant	PSC	-	Liver transplantation, no CCA	2	30	M	Alive
Biliary brush	27	Non-malignant	PSC	-	Liver transplantation, no CCA	2	37	M	Alive
Biliary brush	28a	Non-malignant	PSC	-	-	2	43	M	52
Biliary brush	28b	Non-malignant	PSC	-	-	2	43	M	52
Biliary brush	29	Non-malignant	PSC	-	-	2	30	M	51
Biliary brush	30	Non-malignant	PSC	-	-	2	16	M	49
Biliary brush	31	Non-malignant	PSC	-	-	2	19	M	44
Biliary brush	32	Non-malignant	PSC	-	-	2	62	M	44
Biliary brush	33	Non-malignant	PSC	-	-	2	57	M	41
Biliary brush	34	Non-malignant	PSC	-	-	2	41	M	38
Biliary brush	35	Non-malignant	PSC	-	-	2	47	F	33
Biliary brush	36	Non-malignant	Small-duct PSC	-	-	2	27	M	30
Biliary brush	37	Non-malignant	PSC	-	-	2	45	M	27
Biliary brush	38	Non-malignant	PSC	-	-	2	38	M	27
Biliary brush	39	Non-malignant	PSC	-	-	2	30	M	58
Biliary brush	40	Non-malignant	PSC	-	Liver transplantation, no CCA	2	34	M	Alive
Biliary brush	41	Non-malignant	PSC	-	Liver transplantation, no CCA	2	57	M	Alive
Biliary brush	42	Non-malignant	PSC	-	-	3	20	M	57
Biliary brush	43	Non-malignant	PSC	-	-	3	29	M	51

Biliary brush	44	Non-malignant	PSC	-	-	2	23	M	51
Biliary brush	45	Non-malignant	PBC	-	-	2	48	K	49
Biliary brush	46	Non-malignant	PSC	-	Liver transplantation, no CCA	2	44	F	Alive
Biliary brush	47	Non-malignant	PSC	-	Liver transplantation, no CCA	4	33	M	Alive
Biliary brush	48	Non-malignant	PSC	-	Liver transplantation, no CCA	2	48	M	Alive
Biliary brush	49	Non-malignant	PSC	-	-	2	50	F	50
Biliary brush	50a	Non-malignant	PSC	-	Liver transplantation. Some dysplastic nodules in liver, not HCC	2	35	M	Alive
Biliary brush	50b	Non-malignant	PSC	-	Liver transplantation. Some dysplastic nodules in liver, not HCC	2	35	M	Alive

All biliary brush samples are grouped in numerical order and followed by A and B when multiple samples were obtained from the same patient. Cytology scoring was performed according to published criteria (53): Category 1 was denoted when material was insufficient for analysis. Categories 2 (normal epithelium and/or irregular non-dysplastic changes) and 3 (indefinite for dysplasia) were considered to be negative whereas categories 4 (low-grade dysplasia) and 5 (high-grade dysplasia/adenocarcinoma) were considered to be positive, indicating the presence of CCA. *Cytology was performed on two parallel brushes, and the most severe category was used in comparison with the biomarker-panel.. Abbreviations: CCA, cholangiocarcinoma; CT, computed tomography; ECC, extrahepatic cholagiocarcinoma; ERCP, endoscopic retrograde cholangiopancreatography; F, female; HCC, hepatocellular carcinoma; ICC, intrahepatic cholangiocarcinoma; M, male; MRCP, magnetic resonance cholangiopancreatography; N/A, not available; N/C, not enough cells present for analysis; N/D, no data (most likely due to presence of bacteria and fungi) ; PET, positron emission tomography; PSC, primary sclerosing cholangitis.

Supplementary Table 4. Assays used for quantitative methylation-specific polymerase chain reaction (qMSP)

Assay	Sense primer	Antisense primer	Probe	Frg. size (bp)	Number of assayed CpG sites	Ref.
ALU qMSP	GGTTAGGTATAGTGGTTTATATTTGTA ATTTTAGTA	ATTAACTAAACTAATCTTAAACTCCT AACCTCA	6FAM-CCTACCTTAACCTCCC-MGB	98	-	(54)
CDO1 qMSP	CGAATTATAGCGGCGGAGGT	AAATCGCGTAAACTCCGCG	6FAM-CGTTAGGTCGGGCGGT-MGB	101	10	(1)
CNRIP1 qMSP	TTTAGTTGCGCGGATTTGC	GCACCCGAAAACTCGCTCTA	6FAM-CCGCAAACCGCCG-MGB	55	8	(55)
DCLK1 qMSP	GCGCGTACGCGGAGG	CGACGACGAACGCGCT	6FAM-CGGGAGGGCGTGTGA-MGB	86	11	(1)

FBN1 qMSP	GAGTTATAGTTGGGATAGTTGCGAGC	AACGACGACTCCGACTCCC	6FAM-CGCTACAACCACTACTCGA-MGB	101	8	(55)
INA qMSP	AAAAGTCGGGCGTATCGTTTC	CGACTTCAACGCGAACTACAAA	6FAM-ATACGACAAACAAAACGCGA-MGB	75	10	(55)
MAL qMSP	CGTTTAGGTTATTGGGTTTCGC	CGAACGCCGCTCAAACTC	6FAM-CGCAAACCTCTCGCTAA-MGB	63	8	(55)
SEPT9 qMSP	CGCGCGATTCGTTGTTTATTA	CCAACCCAACACCCACCTT	6FAM-GGATTTCGCGGTTAAC-MGB	98	7	(56)
SFRP1 qMSP	GAATTCGTTCGCGAGGGA	AAACGAACCGCACTCGTTACC	6FAM-CGTCACCGACGCGAA-MGB	70	10	(1)
SNCA qMSP	GCGTTTTGGGCGTTTTTTTAC	CGCTATAAACCGACGACGC	6FAM-CGCTAACCTATCGTCGAA-MGB	143	11	(55)
SPG20 qMSP	GCGCGTCGTGGAACGT	CTACGCTCGCCGAAAACC	6FAM-CGCGCTTACCGTAACAA-MGB	84	10	(55)
TMEFF2 qMSP	GTTCGGGGTTACGCGC	TTCGCCTCACTCTCCGCT	6FAM-TCGGATTTCGTTTTCGGTAG-MGB	83	9	(44)
VIM qMSP	GGTCGAGTTTTAGTCGGAGTTACGT	CCCGAAAACGAAACGTAAAAACTA	6FAM-CGTATTTATAGTTTGGGTAGCGC-MGB	106	9	(19)
ZSCAN18 qMSP	CGCGGTATAGTTTCGCGGTAT	CGCGATAACGACCGACAAA	6FAM-CGTAGTTCGCGGTGAGG-MGB	84	11	(1)

Supplementary Table 5. Individual scoring thresholds used for scoring methylation in the respective sample sets

Type of samples	Sample set	CDO1	CNRIP1	DCLK1	FBN1	INA	MAL	SEPT9	SFRP1	SNCA	SPG20	TMEFF2	VIM	ZSCAN18
Tissue samples	Fresh frozen	1	1	2	1	1	1	1	1	1	1	1	1	1
	FPET	2	1	2	1	1	4	1	5	1	2	4	1	3
Brush samples	Biliary brush	5	3	10	1	1	7	1	7	3	3	6	3	8

The individual scoring thresholds were set based on the highest PMR value in non-malignant controls in the different sample sets. PMR values above the thresholds listed were scored positive for methylation. FPET; formalin-fixed paraffin-embedded tissue.

Supplementary Table 6. Individual methylation sensitivities for all candidate genes in tissue samples

Tissue sample set	CDO1[#]	CNRIP1	DCLK1[#]	FBN1	INA	MAL	SEPT9[*]	SFRP1[#]	SNCA	SPG20	TMEFF2[*]	VIM[*]	ZSCAN18[#]
Fresh frozen samples	85 %	77 %	46 %	31 %	38 %	85 %	25%	69 %	62 %	46 %	67%	42%	77 %
Formalin fixed samples	73 %	85 %	42 %	12 %	27 %	77 %	27%	54 %	15 %	58 %	77%	35%	42 %
All samles	77 %	82 %	44 %	18 %	31 %	79 %	26%	59 %	31 %	54 %	73%	37%	54 %

All methylation sensitivities are listed with 100% specificity. [#] previously published results.(1) [*]Data missing for one CCA.

Supplementary Figure legends

Supplementary Figure 1. Gene expression of a) *CDO1* b) *CNRIP1* c) *SEPT9* and d) *VIM* in publically available CCA and normal samples. RNAseq version 2 data was obtained from the TCGA Research Network (http://cancergenome.nih.gov/), where the samples had been analyzed using the Illumina HiSeq platform. A total of 36 CCAs and nine matching normals were available for analysis. *P*-values were obtained using Mann-Whitney U test (all samples), and wilcoxon rank test (matching samples). *Only values annotated to hg19 were applied.

Supplementary Figure 2. qMSP traces of biliary brush samples. Representative amplification plots of cholangiocarcinomas (left, red) and non-malignant control (right, green) brushings separated according to their Ct-values for a) *CDO1* b) *CNRIP1* c) *SEPT9* and d) *VIM*

Supplementary Figure 3. Comparing the performance of the epi-panel in gallbladder (GBC) and pancreatic (PC) cancer with that of conventional cytology in biliary brush samples. For the epi-panel (*CDO1*, *CNRIP1*, *SEPT9*, and *VIM*) see the following color code: Red; methylated, Green; unmethylated, Gray; no data. For cytology: Closed circle; positive, open circle; negative (scored according to (53)), N/A; not available, N/C; not enough cells present for analysis, N/D; no data.

Supplementary Figure 4. Epi-panel status in corresponding brush and tissue samples. Red; methylation, Green; unmethyled.

Reference List

1. Andresen K, Boberg KM, Vedeld HM, Honne H, Hektoen M, Wadsworth CA, Clausen OP, et al. Novel target genes and a valid biomarker panel identified for cholangiocarcinoma. Epigenetics 2012;7:1249-57.

2. Heafield MT, Fearn S, Steventon GB, Waring RH, Williams AC, Sturman SG. Plasma cysteine and sulphate levels in patients with motor neurone, Parkinson's and Alzheimer's disease. Neurosci Lett 1990;110:216-220.

3. Brait M, Ling S, Nagpal JK, Chang X, Park HL, Lee J, Okamura J, et al. Cysteine dioxygenase 1 is a tumor suppressor gene silenced by promoter methylation in multiple human cancers. PLoS One 2012;7:e44951.

4. McCoy JG, Bailey LJ, Bitto E, Bingman CA, Aceti DJ, Fox BG, Phillips GN, Jr. Structure and mechanism of mouse cysteine dioxygenase. Proc Natl Acad Sci U S A 2006;103:3084-3089.

5. Satsu H, Terasawa E, Hosokawa Y, Shimizu M. Functional characterization and regulation of the taurine transporter and cysteine dioxygenase in human hepatoblastoma HepG2 cells. Biochem J 2003;375:441-447.

6. Jeschke J, O'Hagan HM, Zhang W, Vatapalli R, Calmon MF, Danilova L, Nelkenbrecher C, et al. Frequent inactivation of cysteine dioxygenase type 1 contributes to survival of breast cancer cells and resistance to anthracyclines. Clin Cancer Res 2013;19:3201-3211.

7. De Carvalho DD, Sharma S, You JS, Su SF, Taberlay PC, Kelly TK, Yang X, et al. DNA methylation screening identifies driver epigenetic events of cancer cell survival. Cancer Cell 2012;21:655-667.

8. Prabhu A, Sarcar B, Kahali S, Yuan Z, Johnson JJ, Adam KP, Kensicki E, et al. Cysteine catabolism: a novel metabolic pathway contributing to glioblastoma growth. Cancer Res 2014;74:787-796.

9. Tsuboyama-Kasaoka N, Hosokawa Y, Kodama H, Matsumoto A, Oka J, Totani M. Human cysteine dioxygenase gene: structural organization, tissue-specific expression and downregulation by phorbol 12-myristate 13-acetate. Biosci Biotechnol Biochem 1999;63:1017-1024.

10. Vedeld HM, Andresen K, Eilertsen I, Nesbakken A, Seruca R, Gladhaug I, Thiis-Evensen E, et al. The novel colorectal cancer biomarkers CDO1, ZSCAN18 and ZNF331 are frequently methylated across gastrointestinal cancers. Int J Cancer 2014.

11. Wrangle J, Machida EO, Danilova L, Hulbert A, Franco N, Zhang W, Glockner SC, et al. Functional identification of cancer-specific methylation of CDO1, HOXA9, and TAC1 for the diagnosis of lung cancer. Clin Cancer Res 2014;20:1856-1864.

12. Niehaus JL, Liu Y, Wallis KT, Egertova M, Bhartur SG, Mukhopadhyay S, Shi S, et al. CB1 cannabinoid receptor activity is modulated by the cannabinoid receptor interacting protein CRIP 1a. Mol Pharmacol 2007;72:1557-1566.

13. Lind GE, Kleivi K, Meling GI, Teixeira MR, Thiis-Evensen E, Rognum TO, Lothe RA. ADAMTS1, CRABP1, and NR3C1 identified as epigenetically deregulated genes in colorectal tumorigenesis. Cell Oncol 2006;28:259-272.

14. Lind GE, Danielsen SA, Ahlquist T, Merok MA, Andresen K, Skotheim RI, Hektoen M, et al. Identification of an epigenetic biomarker panel with high sensitivity and specificity for colorectal cancer and adenomas. Mol Cancer 2011;10:85.

15. Bethge N, Lothe RA, Honne H, Andresen K, Troen G, Eknaes M, Liestol K, et al. Colorectal cancer DNA methylation marker panel validated with high performance in Non-Hodgkin lymphoma. Epigenetics 2014;9:428-436.

16. Oster B, Thorsen K, Lamy P, Wojdacz TK, Hansen LL, Birkenkamp-Demtroder K, Sorensen KD, et al. Identification and validation of highly frequent CpG island hypermethylation in colorectal adenomas and carcinomas. Int J Cancer 2011;129:2855-2866.

17. Chong Y, Mia-Jan K, Ryu H, Abdul-Ghafar J, Munkhdelger J, Lkhagvadorj S, Jung SY, et al. DNA methylation status of a distinctively different subset of genes is associated with each histologic Lauren classification subtype in early gastric carcinogenesis. Oncol Rep 2014;31:2535-2544.

18. Moinova H, Leidner RS, Ravi L, Lutterbaugh J, Barnholtz-Sloan JS, Chen Y, Chak A, et al. Aberrant vimentin methylation is characteristic of upper gastrointestinal pathologies. Cancer Epidemiol Biomarkers Prev 2012;21:594-600.

19. Lind GE, Ahmed D, Lothe RA. Vimentin in Upper Gastrointestinal Pathologies - Letter. Cancer Epidemiol Biomarkers Prev 2012;21:1889.

20. Taniguchi H, Yamamoto H, Hirata T, Miyamoto N, Oki M, Nosho K, Adachi Y, et al. Frequent epigenetic inactivation of Wnt inhibitory factor-1 in human gastrointestinal cancers. Oncogene 2005;24:7946-7952.

21. McDade SS, Hall PA, Russell SE. Translational control of SEPT9 isoforms is perturbed in disease. Hum Mol Genet 2007;16:742-752.

22. McIlhatton MA, Burrows JF, Donaghy PG, Chanduloy S, Johnston PG, Russell SE. Genomic organization, complex splicing pattern and expression of a human septin gene on chromosome 17q25.3. Oncogene 2001;20:5930-5939.

23. Sellin ME, Sandblad L, Stenmark S, Gullberg M. Deciphering the rules governing assembly order of mammalian septin complexes. Mol Biol Cell 2011;22:3152-3164.

24. Mostowy S, Cossart P. Septins: the fourth component of the cytoskeleton. Nat Rev Mol Cell Biol 2012;13:183-194.

25. Bennett KL, Karpenko M, Lin MT, Claus R, Arab K, Dyckhoff G, Plinkert P, et al. Frequently methylated tumor suppressor genes in head and neck squamous cell carcinoma. Cancer Res 2008;68:4494-4499.

26. Burrows JF, Chanduloy S, McIlhatton MA, Nagar H, Yeates K, Donaghy P, Price J, et al. Altered expression of the septin gene, SEPT9, in ovarian neoplasia. J Pathol 2003;201:581-588.

27. Connolly D, Yang Z, Castaldi M, Simmons N, Oktay MH, Coniglio S, Fazzari MJ, et al. Septin 9 isoform expression, localization and epigenetic changes during human and mouse breast cancer progression. Breast Cancer Res 2011;13:R76.

28. Gulten T, Yakut T, Karkucak M, Baytan B, Gunes AM. AML1 amplification and 17q25 deletion in a case of childhood acute lymphoblastic leukemia. J Clin Lab Anal 2009;23:368-371.

29. Scott M, Hyland PL, McGregor G, Hillan KJ, Russell SE, Hall PA. Multimodality expression profiling shows SEPT9 to be overexpressed in a wide range of human tumours. Oncogene 2005;24:4688-4700.

30. Scott M, McCluggage WG, Hillan KJ, Hall PA, Russell SE. Altered patterns of transcription of the septin gene, SEPT9, in ovarian tumorigenesis. Int J Cancer 2006;118:1325-1329.

31. Tanaka M, Kijima H, Itoh J, Matsuda T, Tanaka T. Impaired expression of a human septin family gene Bradeion inhibits the growth and tumorigenesis of colorectal cancer in vitro and in vivo. Cancer Gene Ther 2002;9:483-488.

32. Church TR, Wandell M, Lofton-Day C, Mongin SJ, Burger M, Payne SR, Castanos-Velez E, et al. Prospective evaluation of methylated SEPT9 in plasma for detection of asymptomatic colorectal cancer. Gut 2014;63:317-325.

33. Toth K, Galamb O, Spisak S, Wichmann B, Sipos F, Valcz G, Leiszter K, et al. The influence of methylated septin 9 gene on RNA and protein level in colorectal cancer. Pathol Oncol Res 2011;17:503-509.

34. Amir S, Golan M, Mabjeesh NJ. Targeted knockdown of SEPT9_v1 inhibits tumor growth and angiogenesis of human prostate cancer cells concomitant with disruption of hypoxia-inducible factor-1 pathway. Mol Cancer Res 2010;8:643-652.

35. Kakehashi A, Ishii N, Shibata T, Wei M, Okazaki E, Tachibana T, Fukushima S, et al. Mitochondrial prohibitins and septin 9 are implicated in the onset of rat hepatocarcinogenesis. Toxicol Sci 2011;119:61-72.

36. Mendez MG, Kojima S, Goldman RD. Vimentin induces changes in cell shape, motility, and adhesion during the epithelial to mesenchymal transition. FASEB J 2010;24:1838-1851.

37. Mor-Vaknin N, Punturieri A, Sitwala K, Markovitz DM. Vimentin is secreted by activated macrophages. Nat Cell Biol 2003;5:59-63.

38. Sarria AJ, Panini SR, Evans RM. A functional role for vimentin intermediate filaments in the metabolism of lipoprotein-derived cholesterol in human SW-13 cells. J Biol Chem 1992;267:19455-19463.

39. Santos MI, Tuzlakoglu K, Fuchs S, Gomes ME, Peters K, Unger RE, Piskin E, et al. Endothelial cell colonization and angiogenic potential of combined nano- and micro-fibrous scaffolds for bone tissue engineering. Biomaterials 2008;29:4306-4313.

40. Shen WJ, Zaidi SK, Patel S, Cortez Y, Ueno M, Azhar R, Azhar S, et al. Ablation of vimentin results in defective steroidogenesis. Endocrinology 2012;153:3249-3257.

41. Satelli A, Li S. Vimentin in cancer and its potential as a molecular target for cancer therapy. Cell Mol Life Sci 2011;68:3033-3046.

42. Ivaska J. Vimentin: Central hub in EMT induction? Small GTPases 2011;2:51-53.

43. Ulirsch J, Fan C, Knafl G, Wu MJ, Coleman B, Perou CM, Swift-Scanlan T. Vimentin DNA methylation predicts survival in breast cancer. Breast Cancer Res Treat 2013;137:383-396.

44. Costa VL, Henrique R, Danielsen SA, Duarte-Pereira S, Eknaes M, Skotheim RI, Rodrigues A, et al. Three epigenetic biomarkers, GDF15, TMEFF2, and VIM, accurately predict bladder cancer from DNA-based analyses of urine samples. Clin Cancer Res 2010;16:5842-5851.

45. Jung S, Yi L, Kim J, Jeong D, Oh T, Kim CH, Kim CJ, et al. The role of vimentin as a methylation biomarker for early diagnosis of cervical cancer. Mol Cells 2011;31:405-411.

46. Kisiel JB, Yab TC, Taylor WR, Chari ST, Petersen GM, Mahoney DW, Ahlquist DA. Stool DNA testing for the detection of pancreatic cancer: assessment of methylation marker candidates. Cancer 2012;118:2623-2631.

47. Kitamura Y, Shirahata A, Sakuraba K, Goto T, Mizukami H, Saito M, Ishibashi K, et al. Aberrant methylation of the Vimentin gene in hepatocellular carcinoma. Anticancer Res 2011;31:1289-1291.

48. Chen WD, Han ZJ, Skoletsky J, Olson J, Sah J, Myeroff L, Platzer P, et al. Detection in fecal DNA of colon cancer-specific methylation of the nonexpressed vimentin gene. J Natl Cancer Inst 2005;97:1124-1132.

49. Itzkowitz SH, Jandorf L, Brand R, Rabeneck L, Schroy PC, III, Sontag S, Johnson D, et al. Improved fecal DNA test for colorectal cancer screening. Clin Gastroenterol Hepatol 2007;5:111-117.

50. Lao VV, Grady WM. Epigenetics and colorectal cancer. Nat Rev Gastroenterol Hepatol 2011;8:686-700.

51. Baek YH, Chang E, Kim YJ, Kim BK, Sohn JH, Park DI. Stool methylation-specific polymerase chain reaction assay for the detection of colorectal neoplasia in Korean patients. Dis Colon Rectum 2009;52:1452-1459.

52. Ngan CY, Yamamoto H, Seshimo I, Tsujino T, Man-i M, Ikeda JI, Konishi K, et al. Quantitative evaluation of vimentin expression in tumour stroma of colorectal cancer. Br J Cancer 2007;96:986-992.

53. Boberg KM, Jebsen P, Clausen OP, Foss A, Aabakken L, Schrumpf E. Diagnostic benefit of biliary brush cytology in cholangiocarcinoma in primary sclerosing cholangitis. J Hepatol 2006;45:568-574.

54. Weisenberger DJ, Campan M, Long TI, Kim M, Woods C, Fiala E, Ehrlich M, et al. Analysis of repetitive element DNA methylation by MethyLight. Nucleic Acids Res 2005;33:6823-6836.

55. Lind GE, Danielsen SA, Ahlquist T, Merok MA, Andresen K, Skotheim RI, Hektoen M, et al. Identification of an epigenetic biomarker panel with high sensitivity and specificity for colorectal cancer and adenomas. Mol Cancer 2011;10:85.

56. Lofton-Day C, Model F, deVos T, Tetzner R, Distler J, Schuster M, Song X, et al. DNA methylation biomarkers for blood-based colorectal cancer screening. Clin Chem 2008;54:414-423.

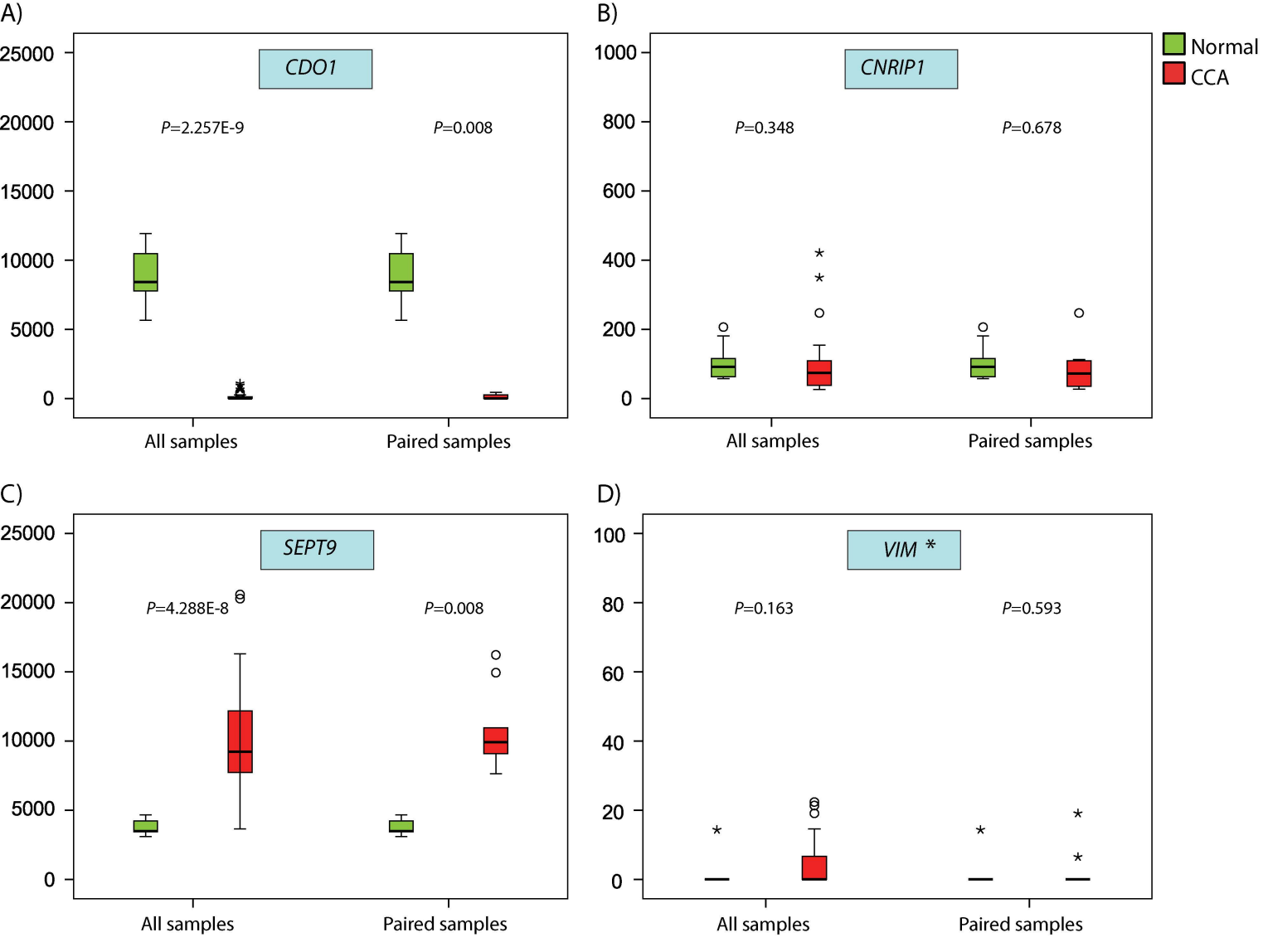
A)
CDO1
P=2.257E-9
P=0.008
25000
20000
15000
10000
5000
0
All samples
Paired samples
B)
CNRIP1
P=0.348
P=0.678
1000
800
600
400
200
0
All samples
Paired samples
Normal
CCA
C)
SEPT9
P=4.288E-8
P=0.008
25000
20000
15000
10000
5000
0
All samples
Paired samples
D)
VIM *
P=0.163
P=0.593
100
80
60
40
20
0
All samples
Paired samples

a)

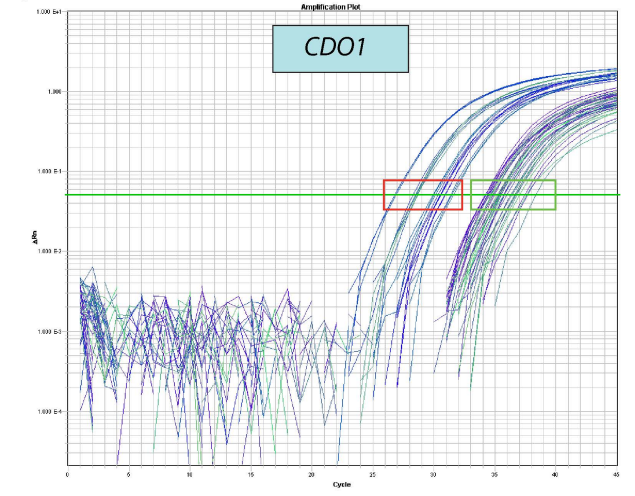
Amplification Plot
CDO1
Cycle

b)

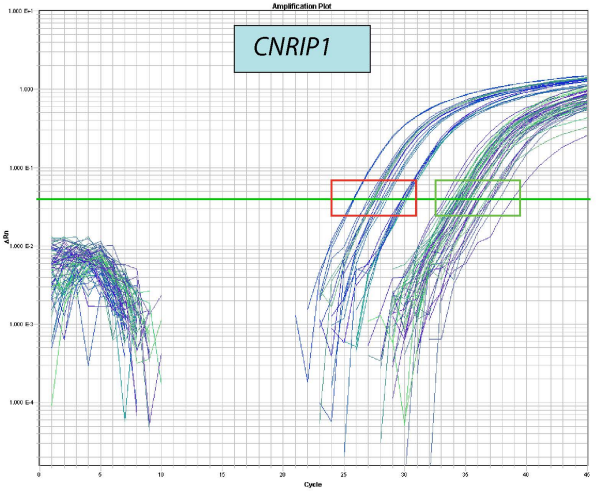
Amplification Plot
CNRIP1
Cycle

c)

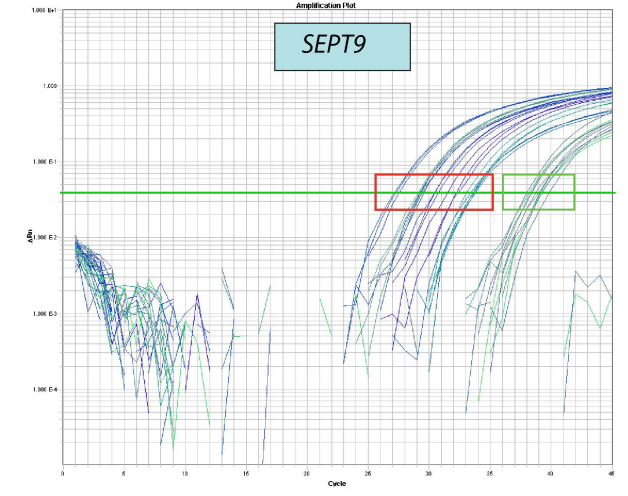
Amplification Plot
SEPT9
Cycle

d)

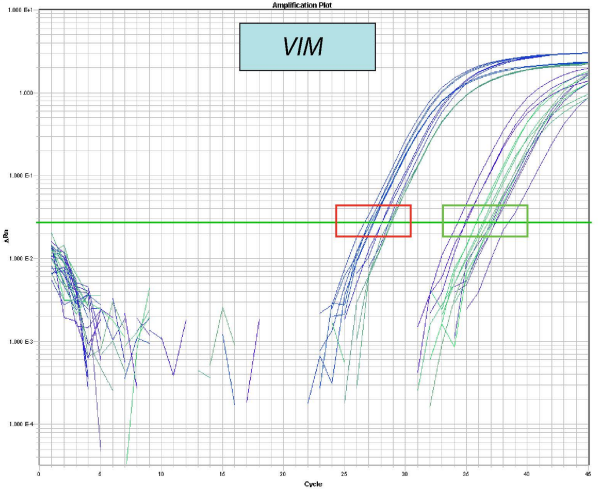
Amplification Plot
VIM
Cycle

	CDO1	CNRIP1	SEPT9	VIM	Biomarker panel	Cytology
GBC						
Sensitivity	75 %	75 %	25 %	25 %	75 %	20 %
Combined sensitivity					60 %	
Specificity	100 %	100 %	100 %	100 %	100 %	100 %
PC	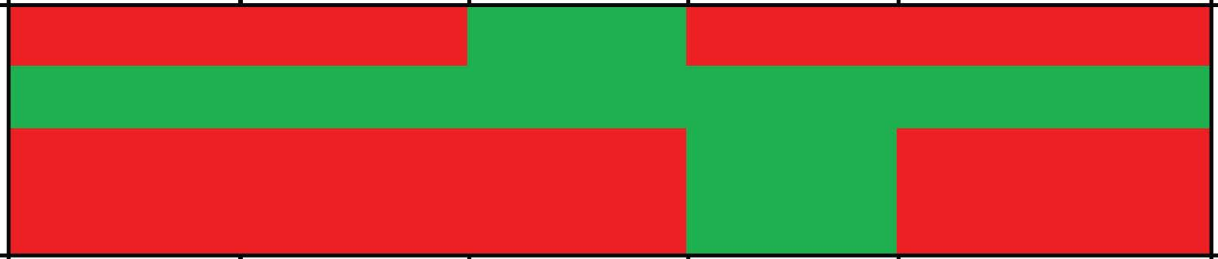					
Sensitivity	75 %	75 %	50 %	25 %	75 %	50 %
Combined sensitivity					100 %	
Specificity	100 %	100 %	100 %	100 %	100 %	100 %

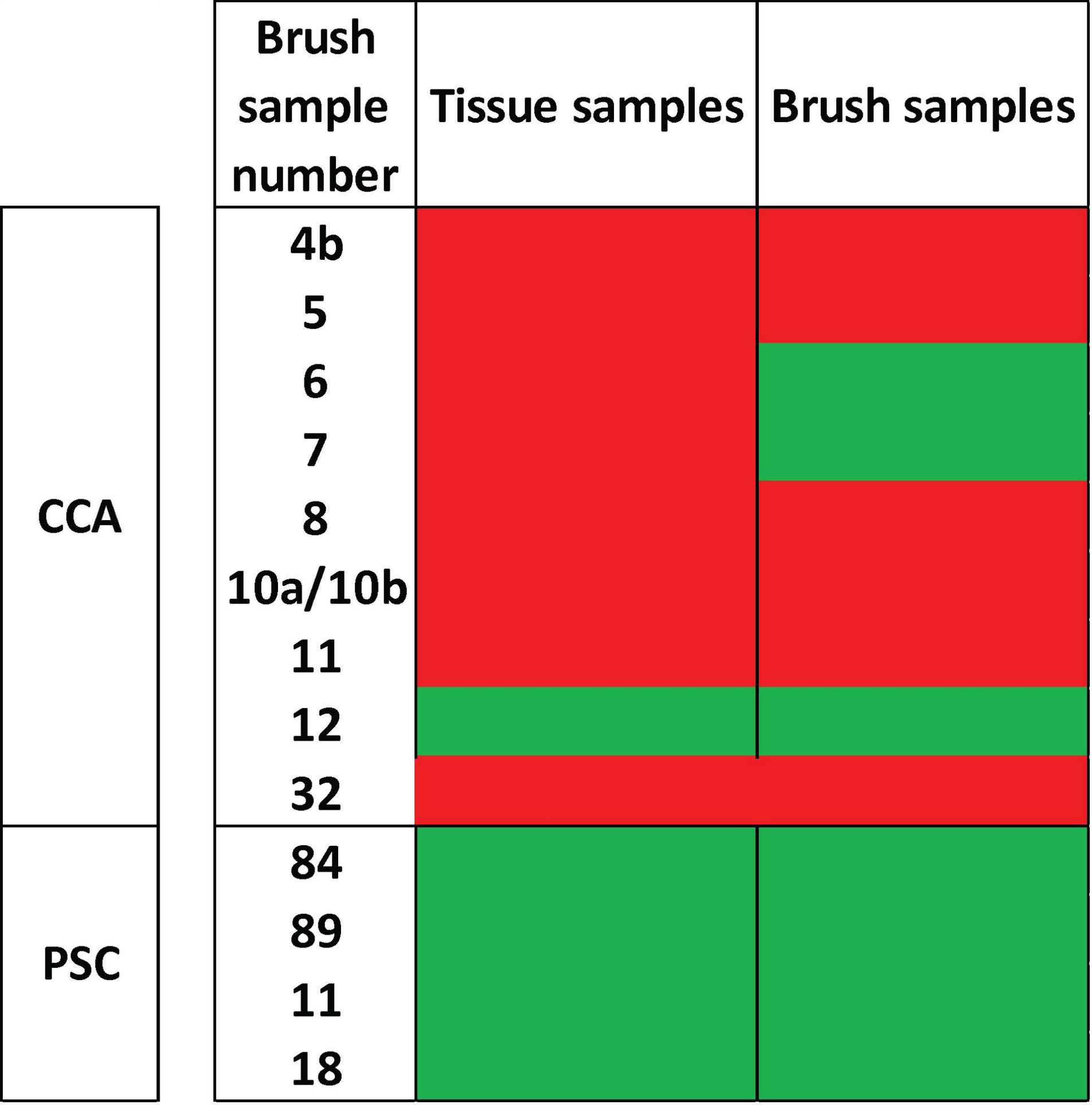
Brush sample number
Tissue samples
Brush samples
CCA
4b
5
6
7
8
10a/10b
11
12
32
PSC
84
89
11
18